

Compositional dependence of refractive index and Raman spectra of $\text{Ge}(\text{S}_x\text{Se}_{1-x})_2$ glasses

JUN ZHANG^{a,b}, HAIYAN XIAO^{a*}, JIE ZHANG^{a,c}

^aState Key Laboratory of Silicate Materials for Architecture (Wuhan University of Technology), Wuhan 430070, P.R.China

^bChina Triumph International Engineering Co., Ltd., Shanghai 200063, P.R. China

^cState Key Laboratory of New Ceramic and Fine Processing (Tsinghua University), Beijing 62772556, China

$\text{Ge}(\text{S}_x\text{Se}_{1-x})_2$ Pseudo-binary chalcogenide glasses with rather wider range from $x=0$ to 1 were obtained through the well-established melt-quenching technique. Utilizing Raman scattering technique, the gradual redistribution of tetrahedral units $[\text{GeS}_{4-n}\text{Se}_n]$ ($n=0, 1, 2, 3$ and 4) in $\text{Ge}(\text{S}_x\text{Se}_{1-x})_2$ glasses following the substitution of Sulfur by Selenium or vice versa were clearly exhibited through the evolution of their characteristic Raman spectral peaks especially in the range of $210 \sim 310\text{cm}^{-1}$, which indicate that the structural units and their cross-linking manner of the $\text{Ge}(\text{S}_x\text{Se}_{1-x})_2$ glasses is basically identical with GeS_2 or GeSe_2 glasses. Based on these micro-structural analysis, the linear evolution of refractive index of these $\text{Ge}(\text{S}_x\text{Se}_{1-x})_2$ glasses together with the gradual blue shift of short-wave absorptive edge λ_{vis} following the substitution of S by Se can be elucidated reasonably.

(Received April 22, 2011; accepted July 25, 2011)

Keywords: Chalcogenide glasses, Raman scattering, Refractive index, $\text{Ge}(\text{S}_x\text{Se}_{1-x})_2$ glasses

1. Introduction

Recently chalcogenide glasses have received increased interest due to their high linear and nonlinear refractive indices and good transmittance into the infrared region. These materials are seen as potential candidates for infrared frequency conversion[1,2], reversible optical recording media[3], inorganic photoresists [4], all-optical switching[5-9] and so forth. Considering the intimate relationship between the properties and structure, structural investigation of chalcogenide glasses has important academic and practical meanings.

In the past decades, much research on the structure of Ge-S and Ge-Se binary glassy systems has been done by Raman scattering technology [10-19]. Raman spectra of GeS_2 and GeSe_2 glasses have been reasonably ascribed. For Ge-S-Se ternary glassy system, several studies [20,21] have been carried out. Structural investigation of substitution of Se by S up to 0.25 for $\text{Ge}(\text{S}_x\text{Se}_{1-x})_2$ glasses verified the existence of mixed tetrahedra $[\text{GeS}_{4-n}\text{Se}_n]$ ($n=1, 2$ and 3). But further study on substitution of Se by S more than 0.25 was not conducted. In this paper, we report the evolution of refractive indices and Raman spectra of $\text{Ge}(\text{S}_x\text{Se}_{1-x})_2$ glasses with much wider compositional range ($0 \leq x \leq 1$). According to the information of Structural evolution obtained from Raman spectra, we elucidated reasonably the origin of evolution of refractive indices of the $\text{Ge}(\text{S}_x\text{Se}_{1-x})_2$ glasses.

2. Experimental procedure

Samples of $\text{Ge}(\text{S}_x\text{Se}_{1-x})_2$ glasses were prepared by conventional melt-quenching technique using high purity

Ge, S, Se (all of 5N) as raw materials. Details of the preparations were similar to the procedure in our previous paper [10,11]. Preparation is conducted following a procedure which consists in mixing the raw materials in the exact appropriate stoichiometry and putting the as-obtained elements into a silica tube to be sealed under vacuum. The ampoules were then placed into a rocking furnace to slowly heat to the temperature of 960°C and hold at this temperature for ~ 12 h. Then the batch is homogenized at a lower temperature according to the composition during 2h before quenching in water or in the ice-water mixture, finally annealing at a temperature slightly lower than T_g . The glass plates were prepared from the bulk glasses and polished to get a mirror surface on both sides.

The amorphous character of $\text{Ge}(\text{S}_x\text{Se}_{1-x})_2$ glasses were verified by X-ray diffraction (XRD) patterns with Cu $K\alpha$ -radiation at an output power 2 kW (40 kV and 40 mA). A UV/VIS/NIR spectrometer (Shimadzu UV-3600) was used to measure the transmission spectrum of the prepared samples.

Raman spectra were measured at room temperature using the back (180°) scattering configuration by the micro Raman Spectrometer (type: inVia) made by Renishaw Company in United Kingdom. A He-Ne laser ($\lambda = 632.8$ nm) with a total power 50 mW was used as an excitation source. To avoid light-induced effects, restrict the temperature rise and obtain clear-cut Raman spectra, a laser power equal to 5 mW ($x=0, 0.2$) and 50 mW ($x=0.4, 0.5, 0.6, 0.8$ and 1) were used, respectively. The resolution of the Raman spectra was 1cm^{-1} .

3. Results

The molar compositions of $\text{Ge}(\text{S}_x\text{Se}_{1-x})_2$ glassy samples are shown in the pseudo-ternary diagram (Fig. 1). Amorphous nature of prepared samples was confirmed by XRD. All glassy samples were optically homogeneous, colors of which vary from deep red through pale red to yellow with increasing the content of sulfur.

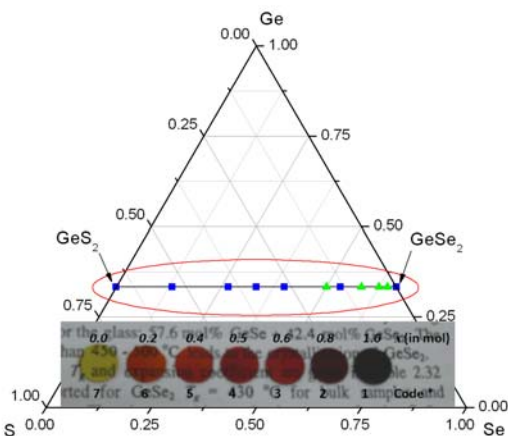


Fig. 1. Ternary Ge-S-Se diagram showing the glass molar compositions investigated in this study (-■-) and in a reference (-▲-)[16]; Inset indicate a optical photo of $\text{Ge}(\text{S}_x\text{Se}_{1-x})_2$ ($0 \leq x \leq 1$) glasses. (* The code are used to express the corresponding $\text{Ge}(\text{S}_x\text{Se}_{1-x})_2$ glass.)

As seen in Fig. 2, the S/Se ratio in the samples influences a lot in short wavelength region. When increasing the content of sulfur the transmittance is enhanced and the short-wavelength cut-off edge (λ_{vis}) shifts to shorter wavelength. In addition, there is a small decrease in the spectral range from 2755 to 3105 nm. It should be attributed to the stretching modes of hydroxyl groups (-OH) which originated from the surface oxidation of the raw materials and the hydroxide contamination during the preparation procedure.

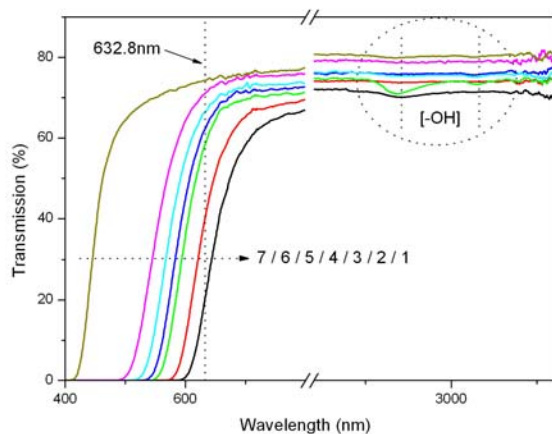


Fig. 2. UV-VIS-NIR transmission spectra of $\text{Ge}(\text{S}_x\text{Se}_{1-x})_2$ glasses.

Within transmission window, provided that absorption

coefficients of glassy samples are equal to zero, then linear refractive index n within NIR transmission window can be calculated by the equation below:

$$n = \frac{(2 - \sqrt{T}) + 2\sqrt{1 - \sqrt{T}}}{\sqrt{T}} \quad (1)$$

where T is the transmittance of glasses. Fig. 3 shows the dispersion curves of refractive index of $\text{Ge}(\text{S}_x\text{Se}_{1-x})_2$ glassy samples within NIR transmission window, calculated by equation (1). Inset indicates the linear evolution of refractive indices of glassy samples at 1064 nm with the change of composition. As to a same component sample, due to chromatic dispersion, n decreases with the increase of wavelength of incident light.

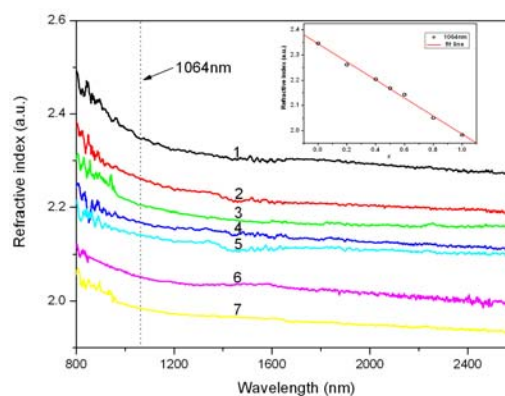


Fig. 3. Dispersion curves of linear refractive indices of $\text{Ge}(\text{S}_x\text{Se}_{1-x})_2$ glasses within NIR transmission window. Inset shows the compositional evolution of refractive indices of $\text{Ge}(\text{S}_x\text{Se}_{1-x})_2$ glasses.

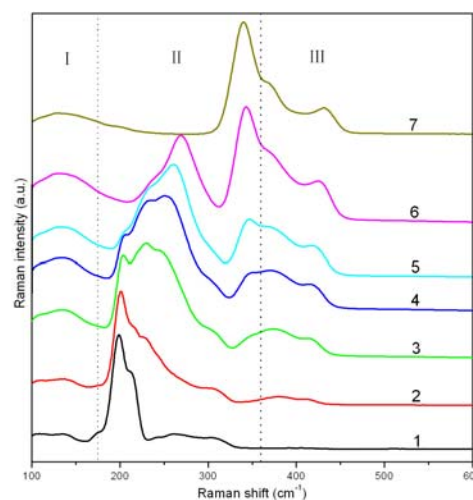


Fig. 4. Raman spectra of $\text{Ge}(\text{S}_x\text{Se}_{1-x})_2$ glasses..

Raman spectra of the $\text{Ge}(\text{S}_x\text{Se}_{1-x})_2$ glassy samples at

room temperature are shown in Fig. 4, in which the spectra are normalized according to the maximum intensity. The evolution of broader prominence in the lower frequency range below 170 cm^{-1} , which maybe ascribed to the bond bending modes of structural units such as $[\text{GeS}_4]$, $[\text{GeSe}_4]$ or mixed $[\text{GeS}_n\text{Se}_{4-n}]$ tetrahedra, is not so clear. Surely, these modes are theoretically expected to be much less intense, broader and less well defined than the symmetric stretching vibrational mode coming out in the spectral range from 180 to 360 cm^{-1} range. Similarly, considering their faint feature in the spectral range higher than 360 cm^{-1} in this work, we will focus on the evolution of spectral evolution in the range between 180 and 360 cm^{-1} . In fact, the stretching vibrational mode of the tetrahedral structural units such as $[\text{GeS}_4]$, $[\text{GeSe}_4]$ or mixed $[\text{GeS}_n\text{Se}_{4-n}]$ tetrahedra exists in this range. And these modes can be seen as useful identified features which will offer clear information about the evolution of basic structural units following the change of ratio of S to Se among $\text{Ge}(\text{S}_x\text{Se}_{1-x})_2$ glasses.

4. Discussion

To preserve valence and coordination requirements, each germanium atom should bond to four chalcogenide atoms and each chalcogenide to two germaniums. Based on this consideration, the network of $\text{GeS}(\text{orSe})_2$ glasses is generally believed to be composed of $[\text{GeS}(\text{orSe})_4]$ tetrahedra which are bridged to each other [12-19]. On the Raman spectra of $\text{GeS}(\text{orSe})_2$ glasses, it is well accepted that the strongest peaks at 340 (or 198) cm^{-1} should be attributed to the symmetric stretching vibrational mode of $[\text{GeS}(\text{orSe})_4]$ tetrahedra. Considering the weaker coupling between $[\text{GeS}(\text{orSe})_4]$ tetrahedra in $\text{GeS}(\text{orSe})_2$ glasses, this symmetric stretching vibrational mode should be easily identified by their relatively narrow-band contours, large scattering strengths, and low depolarization ratios. Considering the similarity of atomic weight of S (or Se) and Cl (or Br), through the analogy of characteristic lines of Raman spectra of mixed $\text{GeCl}_n\text{Br}_{4-n}$ ($n=0,1,2,3,4$) tetrahedra among the mixed GeCl_4 and GeBr_4 liquid or gaseous, which has been well established, the corresponding so-called ν_1 mode of the mixed $[\text{GeS}_n\text{Se}_{4-n}]$ ($n=0,1,2,3,4$) tetrahedra among $\text{Ge}(\text{S}_x\text{Se}_{1-x})_2$ glasses was predicted to exist and locate at about 222 ($n=1$), 243 ($n=2$), and 266 ($n=3$) cm^{-1} and was further confirmed utilizing the Raman spectra of $\text{Ge}(\text{S}_x\text{Se}_{1-x})_2$ glasses ($x=0\sim 0.25$) by Griffiths et al [20].

On one side, following the addition of sulfur in $\text{Ge}(\text{S}_x\text{Se}_{1-x})_2$ glasses, as seen in Fig.4(1 to 2), the characteristic peaks of mixed tetrahedra $\text{GeS}_n\text{Se}_{4-n}$ begin to come out and their intensity distribution indicates the gradually decreasing quantity according to the following order $[\text{GeSe}_4]$, $[\text{GeSe}_3\text{S}]$, $[\text{GeSe}_2\text{S}_2]$, $[\text{GeSeS}_3]$, but no appearance of GeS_4 tetrahedra, which agree rather well with the previous investigation [20]. However, maybe due to their improper preparation technology, Griffiths et al can not obtain glassy samples in $\text{Ge}(\text{S}_x\text{Se}_{1-x})_2$ system when x is higher than 0.25 .

The strongest characteristic peaks of mixed tetrahedra $[\text{GeSe}_3\text{S}]$, $[\text{GeSe}_2\text{S}_2]$ and $[\text{GeSeS}_3]$ located in the spectral region $210\sim 310\text{ cm}^{-1}$. For Se-rich $\text{Ge}(\text{S}_x\text{Se}_{1-x})_2$ glasses,

considering the superposition of these strongest characteristic peaks with other stronger Raman peaks (for example, the companion mode (212 cm^{-1}) of GeSe_4 tetrahedra originated from the vibrations of bridging selenium Ge_2Se_6 units; the mode at $242, 261\text{ cm}^{-1}$ due to vibrations of T_2 - $[\text{GeSe}_4]$ or $[\text{Se}_n]$ chains), it is not so easy to observe the evolution of characteristic peaks of mixed $\text{GeS}_n\text{Se}_{4-n}$ tetrahedra. However, for GeS_2 glasses, a very smooth curve (no clear characteristic peaks) comes out in this region. Therefore, the preparation of S-rich $\text{Ge}(\text{S}_x\text{Se}_{1-x})_2$ glasses is very desired considering the above-mentioned facts. Really, through the improved preparation process, the $\text{Ge}(\text{S}_x\text{Se}_{1-x})_2$ glassy samples with wider range from 0 to 1 were obtained in our lab.

As shown in Fig.4 from sample 7 down to sample 3, the evolution of intensity redistribution of the characteristic modes of $\text{GeS}_n\text{Se}_{4-n}$ ($n=0,1,2,3,4$) tetrahedra can be clearly seen following the gradual substitution of Sulfur by Selenium through the addition of Se little by little. First, it is interesting to compare the spectra between sample 2 and 6 considering the addition of an equal quantity of Sulfur or Selenium (20 atomic per cent). The ratio of intensity of characteristic peak of mixed tetrahedral GeSeS_3 to GeSe_2S_2 is much higher than the corresponding one of GeSe_3S to GeSe_2S_2 units, considering the overlap of characteristic peaks of GeSe_3S and bridged Ge_2Se_6 units. On the other hand, when the quantity of addition of S or Se into $\text{Ge}(\text{S}_x\text{Se}_{1-x})_2$ glasses is higher than 40 atomic per cent, the intensity of characteristic peaks of mixed tetrahedra $\text{GeS}_n\text{Se}_{4-n}$ ($n=1,2,3$) will predominant compared with the ones of $[\text{GeS}_4]$ or $[\text{GeSe}_4]$ tetrahedra.

In summary, $[\text{GeS}_n\text{Se}_{4-n}]$ ($n=0\sim 4$) tetrahedra are the basic structural units of $\text{Ge}(\text{S}_x\text{Se}_{1-x})_2$ glasses. Changes of ratio of S to Se can lead to the redistribution of quantity of mixed $\text{GeS}_x\text{Se}_{4-x}$ tetrahedra, but the basic tetrahedral configuration of glassy network is preserved. Based on these facts, it can be deduced that the glassy network of $\text{Ge}(\text{S}_x\text{Se}_{1-x})_2$ glasses can be seen as a crosslink of $[\text{GeS}_n\text{Se}_{4-n}]$ ($n=0\sim 4$) tetrahedra in a similar manner with GeS_2 or GeSe_2 glasses and Se and S atoms are uniformly distributed in this network mainly through hetero-polar bonds.

Clearly blue shift of λ_{vis} of $\text{Ge}(\text{S}_x\text{Se}_{1-x})_2$ glassy samples shown in Fig.2, which is in good agreement with the picture shown in Fig.1, can be interpreted reasonably according to the redistribution of structural units following the addition of Sulfur, considering the gradually increasing band-gap in terms of the augment of n value in $[\text{GeS}_n\text{Se}_{4-n}]$ ($n=0\sim 4$) mixed tetrahedra [21]. In addition, due to the similarity of micro-structural units and crosslink configuration of glassy network in $\text{Ge}(\text{S}_x\text{Se}_{1-x})_2$ glasses, the change of refractive index should be affected only through the substitution of S by Se, which certainly lead to a simple linear evolution as shown in Fig.3.

5. Conclusions

Glassy samples along the GeS_2 - GeSe_2 axis have been studied within the Ge-S-Se ternary diagram. The λ_{vis} displays a gradual blue shift with the increasing ratio of S to Se which is coincident with the change of sample color

from deep red through pale red to yellow; meanwhile, the transmittance is enhanced in near infrared region. With the gradual addition of sulfur, the refractive index of Ge(S_xSe_{1-x})₂ glassy samples decreases linearly. The redistribution of [GeS_nSe_{4-n}] (n=0~4) tetrahedra in Ge(S_xSe_{1-x})₂ glasses with wider range from x=0 to 1 are clearly exhibited through the gradual spectral evolution based on the Raman scattering technique, which indicate that the network of Ge(S_xSe_{1-x})₂ glasses is basically identical with the one of GeS₂ or GeSe₂ glasses.

Acknowledgements

This work was partially funded by NSFC (no., 60808024), Innovative Research Team Project of Hubei Province (2010CDA070). The authors take great pleasure in acknowledging valuable discussions with Haizheng Tao (Wuhan University of Technology).

References

- [1] H.Z. Tao, C.G. Lin, S.X. Gu, C.B. Jing, X.J. Zhao, *Appl. Phys. Lett.* **91**, 011904 (2007).
- [2] Lin CG, Tao HZ, Zheng XL, Pan RK, Zang HC, Zhao XJ, *Opt. Lett.* **34**(4), 437 (2009).
- [3] H.Z. Tao, Z.Y. Yang, P. Lucas, *Opt. Express* **17**, 18165 (2009).
- [4] C.J. Hill, L.H. Huang, A. Jha, *J. Mater. Sci. - Mater. Electron.* **20**, S202 (2009).
- [5] H.Z. Tao, C.G. Lin, S. Mao, G.P. Dong, X.J. Zhao, *J. Non-Cryst. Solids*, **354**(12-13), 1303 (2008).
- [6] H.Z. Tao, S. Mao, W. Tong, X.J. Zhao, *Mater. Lett.*, **60**(6) 741 (2006).
- [7] X. Zheng, F. Chen, H. Tao, et al, *J. Optoelectron. Adv. Mater.* **13**(1-2), 24 (2011).
- [8] H.Z. Tao, G.P. Dong, Y.B. Zhai, H.T. Guo, X.J. Zhao, Z.W. Wang, S.S. Chu, S.F. Wang, Q.H. Gong, *Solid State Commun.* **138** (10-11) 485 (2006).
- [9] G.P. Dong, H.Z. Tao, X.D. Xiao, C.G. Lin, Y.Q. Gong, X.J. Zhao, S.S. Chu, S.F. Wang, Q.H. Gong, *Opt. Express*, **15** (5)2399 (2007).
- [10] R.K. Pan, H.Z. Tao, H.C. Zang, X.J. Zhao, T.J. Zhang, *J. Alloys Compd.* **484**(1-2), 645 (2009).
- [11] R.K. Pan, H.Z. Tao, H.C. Zang HC, X.J. Zhao, T.J. Zhang, *Appl. Phys. A: Mater. Sci.* **99**(4), 889 (2010).
- [12] Y. Wang, K. Tanaka, T. Nakaoka, K. Murase, *J. Non-Cryst. Solids* **299**, 963 (2002).
- [13] P. Lucas, E.A. King, O. Gulbiten, J.L. Yarger, E. Soignard, B. Bureau, *Phys. Rev. B* **80**, 214114-1 (2009).
- [14] P. Boolchand, X. Feng, W.J. Bresser, *J. Non-Cryst. Solids* **293**, 348 (2001).
- [15] H.Z. Tao, X.J. Zhao XJ, C.B. Jing, H. Yang, S. Mao, *Solid State Commun.* **133**(5) 327 (2005).
- [16] C.G. Lin, H.Z. Tao, Z. Wang, B. Wang, X.L. Zheng, H.C. Zang, X.J. Zhao, *J. Non-Cryst. Solids* **355**(7), 438 (2009).
- [17] H.Z. Tao, X.J. Zhao, C.B. Jing, *J. Mol. Struct.* **697**, 23 (2004).
- [18] H.Z. Tao, C.G. Lin, Y.Q. Gong, S. Mao, X.J. Zhao, *Optoelectron. Adv. Mater. - Rapid Comm.* **2**(1), 29 (2008).
- [19] H.Z. Tao, X.J. Zhao, C.B. Jing, S. Liu, *J. Wuhan Univ Technol - Mater. Sci. Ed.* **20**(3), 8 (2005).
- [20] J.E. Griffiths, G.P. Espinosa, J.C. Phillips, J.P. Remeika, *Phys. Rev. B* **28**, 4444 (1983).
- [21] C.C. Wu, C.H. Ho, J.Y. Wu, S.L. Lin, Y.S. Huang, *J. Cryst. Growth* **281**, 377 (2005).

*Corresponding author: xhyl@whut.edu.cn